

Supplementary material

Signaling mechanisms of LOV domains: New insights from molecular dynamics studies

Peter L. Freddolino, Kevin H. Gardner and Klaus Schulten

Reparameterization of FMN and FMN-cysteine photoadduct

The present study makes use of a reparameterization of the flavin mononucleotide chromophore and flavin-cysteinylyl photoadduct; corresponding CHARMM-compatible topology and parameter files are provided as Supplementary Material items 2 and 3. In general, we followed as closely as possible the CHARMM27 strategy for nucleic acid parameterization outlined in Foloppe & MacKerrell Jr¹. All quantum mechanical calculations were performed using GAMESS version 7 SEP 2006 (R4)³. *Ab initio* calculations were carried out at the B3LYP/6-31G* level of theory unless otherwise noted, and geometry optimizations performed to a relative tolerance of 10^{-7} .

All Lennard-Jones parameters were taken by analogy to similar atoms from the CHARMM27 force field. Bonded parameters and charges for the ribose and phosphate moieties were obtained from corresponding CHARMM27 model compounds (ethanol, methanol, and methylphosphate). For the isoalloxazine ring, we used lumiflavin (isoalloxazine with a single methyl group at the N10 position) as a model compound for all parameterization calculations for flavin mononucleotide, and lumiflavin bonded to methanethiol at the C4A position as a model for the FMN-cysteine photoadduct. Bond and angle parameters were calculated directly from the Hessian matrix at the optimized geometry. Equilibrium angles were adjusted as needed to yield a sum of 360 degrees for sets of angles centered on a single ring atom, and 720 degrees for sets of angles around a single six membered ring. Dihedral and improper angle equilibrium values were obtained from the optimized flavin geometries, but force constants obtained by analogy to existing CHARMM27 nucleic acid parameters whenever possible. Improper involving the C4A atom in the photoadduct state were instead parameterized by fitting the CHARMM improper potential to energies from a set of seven structures differing by movements of the C4A atom perpendicular to the plane of the isoalloxazine ring at 0.1 Å increments while keeping the remainder of the geometry fixed.

Partial charges were likewise assigned following CHARMM nucleic acid parameterization procedures with minor variations. For each hydrogen bond donor/acceptor (N1, O2, N3, O4, N5), an optimized interaction distance (and corresponding interaction energy) with all other degrees of freedom fixed was calculated for a water molecule interacting with the ring system at the HF/6-31G* level of theory; the full set of considered interactions is shown in Figure S11. For each interaction the resulting distance and energy from electronic structure calculations were reduced by 0.15 Å and scaled by 1.16, respectively, to obtain target values for the classical parameterization. Force field energies and distances for candidate partial charge distributions were calculated by performing 20,000 steps of conjugate gradient minimization on the structure with all degrees of freedom except the water-isoalloxazine hydrogen bond distance in question strongly restrained. Initial charges were taken from Freddolino *et al.*², and manually tuned to resemble standard CHARMM nucleic acid partial charges and to match CHARMM conventions for groups with predefined partial charges (*e.g.*, methyl groups). We then performed an optimization in partial charge space (with the aforementioned predefined groups fixed), attempting to minimize a weighted sum of three quantities: (i) the magnitude of the weighted sum of the difference between the classical and quantum mechanical dipole moments of the isoalloxazine ring; (ii) the sum of the magnitudes of the differences in interaction distance for all water sites in the quantum mechanical vs. classical descriptions; and (iii) the sum of the magnitudes of the differences in interaction energy for all water sites in the quantum mechanical vs. classical descriptions. Iterative cycles of manual refinement and steepest descent optimization to minimize the objective function were applied, ending with automated optimization. The final partial charge sets have a difference in dipole moment less than 15% in magnitude from the quantum mechanical dipole moment, and no deviation in water-isoalloxazine interaction energy or distance greater than 10% of the classical value.

Supplementary Figures

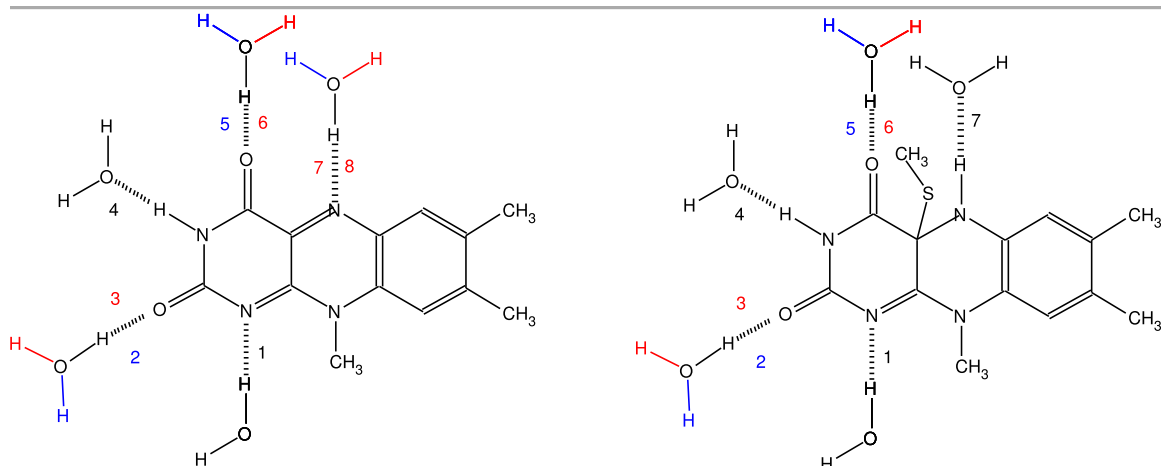


Figure S11: Ring-water interactions used to parameterize the partial charges of the isoalloxazine moiety. Only the dashed distances were considered, as described in the text. Interactions are shown for the normal (left) and photoadduct (right) states of the molecule.

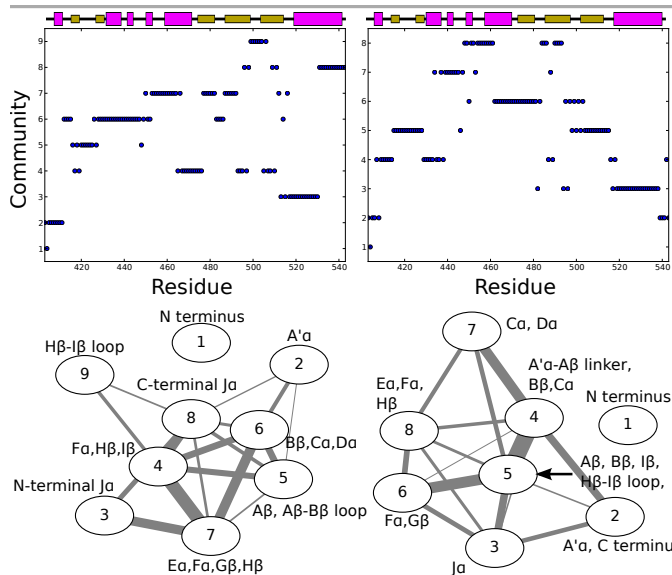


Figure S12: Network analysis results analogous to those in the main text, using the center of mass of each residue rather than its alpha carbon for correlation calculations. Results for the dark and light state are shown on the left and right, respectively; in each case, we display community membership (top) and interactions between communities (bottom) equivalent to those in Fig. 5 of the main text.

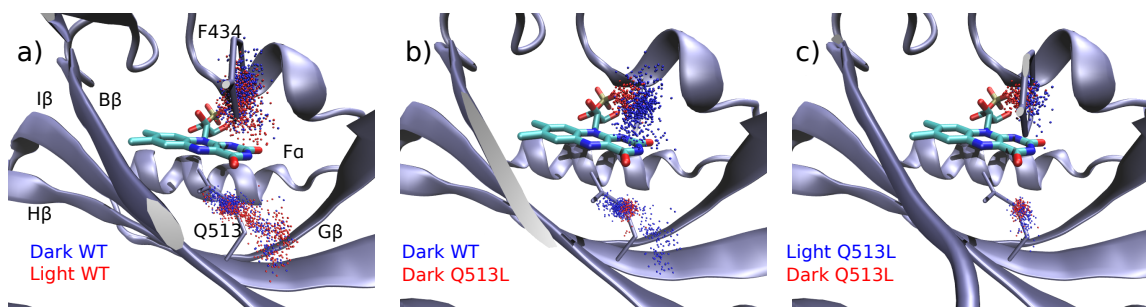


Figure SI3: Conformational distribution of F434 and Q/L513 in the wild type protein and Q513L mutant. In each case, the starting conformation of the protein backbone, FMN, and residues of interest are shown, and then colored spheres indicate the positions of the side chain center of mass for the two atoms of interest in a series of snapshots separated by 1 ns, from all portions of the relevant trajectories after the initial 80 ns. (a) Comparison of WT dark state (blue) and light state (red) simulations. (b) Comparison of wild type dark state simulations (blue) with Q513L dark state simulations (red). (c) Comparison of Q513L dark state simulations (red) with Q513L light state simulations (blue). We did not observe notable changes in the conformations of other residues in the FMN binding site during the Q513L trajectories.

Supplementary Movies

Movies SI1 and SI2: Rotating views of the clusters presented in Figure 3, showing results from the dark state (Movie SI1) and light state (Movie SI2). Conformations of the first six clusters from equilibrium MD trajectories are shown in solid cartoons, along with the dark state crystal structure of the appropriate state is shown in a grey transparent representation for reference.

References

- [1] Foloppe, N. & MacKerrell Jr., A. D. 2000 All-atom empirical force field for nucleic acids: I. parameter optimization based on small molecule and condensed phase macromolecular target data. *J. Comp. Chem.*, **21**, 86–104.
- [2] Freddolino, P. L., Dittrich, M. & Schulten, K. 2006 Dynamic switching mechanisms in LOV1 and LOV2 domains of plant phototropins. *Biophys J*, **91**(10), 3630–3639.
- [3] Schmidt, M., Baldrige, K., Boatz, J., Elbert, S., Gordon, M., Jensen, J., Koseki, S., Matsunaga, N., Nguyen, K. *et al.* 1993 General atomic and molecular electronic structure system. *J. Comput. Chem.*, **14**, 1347–1363.